Analytical optimal controls for the state constrained addition and removal of cryoprotective agents

James D. Benson · **Carmen C. Chicone** · **John K. Critser***

Abstract Cryobiology is a field with enormous scientific, financial and even cultural impact. Successful cryopreservation of cells and tissues depends on the equilibration of these materials with high concentrations of permeating chemicals (CPAs) such as glycerol or 1,2 propylene glycol. Because cells and tissues are exposed to highly anisosmotic conditions,

---

*Corresponding Author

James D Benson

Applied and Computational Mathematics Division

National Institute of Standards and Technology

Gaithersburg, MD 20879

Carmen C. Chicone

Department of Mathematics

University of Missouri

Columbia, MO, 65211

John K. Critser

Department of Veterinary Pathobiology

University of Missouri

Columbia, MO, 65211

the resulting gradients cause large volume fluctuations that have been shown to damage cells and tissues. On the other hand, there is evidence that toxicity to these high levels of chemicals is time dependent, and therefore it is ideal to minimize exposure time as well. Because solute and solvent flux is governed by a system of ordinary differential equations, CPA addition and removal from cells is an ideal context for the application of optimal control theory. Recently, we presented a mathematical synthesis of the optimal controls for the ODE system commonly used in cryobiology in the absence of state constraints and showed that controls defined by this synthesis were optimal. Here we define the appropriate model, analytically extend the previous theory to one encompassing state constraints, and as an example apply this to the critical and clinically important cell type of human oocytes, where current methodologies are either difficult to implement or have very limited success rates. We show that an enormous increase in equilibration efficiency can be achieved under the new protocols when compared to classic protocols, potentially allowing a greatly increased survival rate for human oocytes, and pointing to a direction for the cryopreservation of many other cell types.

Keywords cryobiology · optimal control · cryoprotective agent · mass transfer

Introduction

The economic, scientific and even cultural impact of cryobiology is immense[1]: billions of dollars are invested in frozen cells and tissues for use in cell culture transport [4], facilitation of agricultural and human reproduction [31], improvements in human and animal medicine [25], and bioengineering [19]. Arguably more important than cooling and warming rates, the addition and removal of cryoprotective agents (CPAs) to and from cells [26] is a critical and

---

[1] Part of this work appeared as part of a doctoral dissertation [5]

limiting factor in cryopreservation success—current cryopreservation protocols are limited by the inability to equilibrate cells with sufficiently high concentrations of CPAs to cause an intracellular glass to form while cooling. The transport of CPAs across cell membranes is well described by a system of coupled nonlinear ordinary differential equations, and is often limited by the existence of cell-specific volume or concentration constraints [26]. To date only heuristic optimizations of CPA addition and removal protocols have been published [14,24,23]. Here we show that optimal control theory can be successfully applied to the introduction and subsequent removal of cryoprotective agents. Moreover, while applying the general optimization theory outlined recently [7], we are able to add the natural cell volume and concentration constraints that are encountered in the process of cryoprotective agent addition and removal [4]. Here we show that for a large set of parameters, at least a five-fold time reduction can be made over classical techniques. We then provide a specific application to human oocytes, where the time to safely equilibrate oocytes with vitrification level ethylene glycol (e.g. more than 40 molal) is reduced by a factor of five to twenty.

There are two conflicting factors in the development of a CPA addition or removal protocol—the exposure time to multimolal concentrations of CPAs and damaging cell and water volume excursions (Fig. 1)—which point to the existence of an optimal protocol and necessitate an algorithm that provides the optimized CPA addition and removal procedure when the membrane permeability characteristics and the osmotic or volumetric tolerance limits of a specific cell type are known. Often CPAs are added and removed in gradual steps, whose durations and concentrations are empirically based [16]. Heuristic methods for the optimization of CPA addition and removal, deriving protocols where the CPA concentration is varied continuously [23,24]. These protocols have produced improved but not optimal protocols limited in the general applicability of the technique.

We wish to control the extracellular concentrations of permeating and non-permeating solutes (M_2 and M_1, respectively) such that cells are equilibrated at a goal state in the shortest time while remaining within predefined state-constraints. For analytical simplicity we will use the solute-solvent transmembrane flux model described by Jacobs [18] and commmonly used in cryobiology [21]. This model recently was noted to encompass a vary large array of membrane transport phenomena [17]. After simplifying the osmotic pressure to a single term in a virial expansion and non-dimensionalizing (cf. [20]) we have the system

$$
\begin{aligned}
\frac{dw}{d\tau} &= M_1 + M_2 + \frac{x_{\mathrm{np}} + S}{w}, \\
\frac{dS}{d\tau} &= b\left(M_2 + \frac{S}{w}\right),
\end{aligned}
\tag{1}
$$

where w and S are the intracellular water volume and moles of solute, respectively, x_{np} is the (assumed fixed) moles of nonpermeating solute, b is a unitless relative permeability constant, and τ is a dimensinless temporal variable. Following an approach we have previously described [6], we factor out w^{-1} to facilitate a time-transform with

$$
s = q(t) := \int_0^t x_1(\xi)d\xi,
\tag{2}
$$

resulting in a system that is linear in the concentration and state variables (see Table 2 for parameter definitions):

$$
\begin{aligned}
\dot{x}_1 &= (M_1 + M_2)x_1 - x_2 + x_{\mathrm{np}}, \\
\dot{x}_2 &= bM_2x_1 - bx_2.
\end{aligned}
\tag{3}
$$

Optimal control

We set $\bar{M}_i > 0$ for $i = 1, 2$, the admissible control parameter set

$$
\mathrm{CP} = \{M = (M_1, M_2) \in \mathbb{R}^2 : 0 \le M_i \le \bar{M}_i \text{ for } i = 1, 2\},
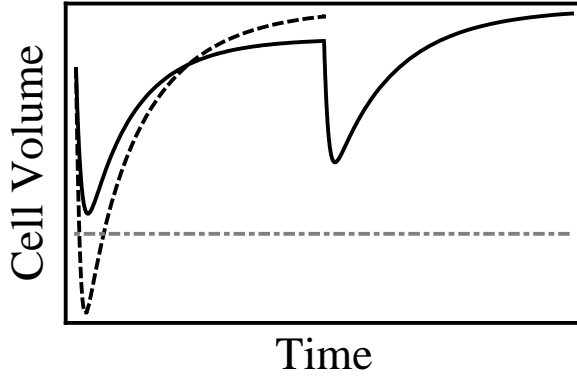\tag{4}
$$

Fig. 1 Plot of the effects of two different CPA addition protocols. A hypothetical cell is equilibrated with a goal concentration C of a permeating CPA. This cell has a lower limit to which it can contract without damage. If the cell is exposed abruptly to C, the efflux of water causes it to shrink below this limit, causing cell death. Alternatively, if the cell is exposed to $C/2$ and then C, the cell does not exceed the limit, but is exposed to the chemicals for a longer period of time. We wish to find an optimal balance between these two competing effects.

and the state space $S \subset (0,\infty) \times [0,\infty)$ (note $x_1 > 0$). In addition, we define $x(t) = x(t; x_0, M)$ to be the solution of the initial value problem (3) and

$$\mathscr{C}_y(t) = \{x_0 \in S : x(t) := x(t; x_0, u) = y\},$$

to be the set of initial conditions that can be steered to $y \in S$ at time t via a measurable, admissible control function $M : \mathbb{R}^+ \to \mathrm{CP}$.

We have a time-optimal control problem of steering an initial state x^i to a final state x^f in minimal "real" time using controls in the admissible set $\mathbb{A}$, the set of measurable functions $M : \mathbb{R} \to \mathrm{CP}$, and formally we may now define the optimal control problems:

Problem 1 Given an initial state w^i in the state space S and final state $w^f \in S$, the set of admissible controls $\mathbb{A}$ and defining $s^* \in \mathbb{R}$ to be the first time that $w(s^*) = w^f$ for the solution of the previously defined initial value problem defined in system (1), determine a control that minimizes s^* over $M \in \mathbb{A}$, subject to constraints $\Gamma \cdot w + k \leq 0$.

Table 1 Definition of parameters

Variable	Non-dimensional parameter description
x_1	Cell water volume
x_2	Cell permeating solute mass
x_{np}	Cell non-permeating solute mass
x^i or x^f	Initial or final state values, respectively
M_1	Extracellular non-permeating solute concentration
M_2	Extracellular permeating solute concentration
$\bar{M}_i$	Maximal solute concentration
b	Unitless relative cell permeability parameter
γ	Partial molar volume of the permeating solute
k	Upper or lower cell volume limit
τ, t_1, t_2	Switching times

Using the time-transform function q in (2), we have the equivalent problem

Problem 2 Given an initial state x^i in the state space S and final state $x^f \in S$, the set of admissible controls $\mathbb{A}$ and defining $t^* \in \mathbb{R}$ to be the first time that $x(t^*) = x^f$ for the solution of the previously defined initial value problem

$$\dot{x} = f(x, M) = A(M)x + x_{np}e_1, \quad x(0) = x^i, \tag{5}$$

determine a control that minimizes the cost functional

$$J(M) := s^* = q(t^*) = \int_0^{t^*} x_1(t)\, dt \tag{6}$$

over $\mathbb{A}$, subject to constraints $\Gamma \cdot w + k \leq 0$.

Table 2 Definition of controls

Control	$M_1(t)$	$M_2(t)$
M^I	0	$\bar{M}_2$
M^{II}	0	0
M^{III}	$\bar{M}_1$	0

Here $\Gamma = (\gamma_1, \gamma_2)^T \in \mathbb{R}^2$ allows the representation of water volume, total cell volume, or concentration in terms of x_1 and x_2. The existence of an optimal control along with the equivalence of these problems is proved in [7].

Though numerical approaches exist for solving Problem 2 with nonlinear and multiple state constraints using classical numerical optimal control techniques, here we will construct analytically the optimal control in the most commonly encountered case where there are total cell volume constraints of the form $k_* \leq x_1 + \gamma_2 x_2 \leq k^*$ corresponding to upper and lower osmotic tolerance limits, where the initial and final water volumes are equal, i.e. $x_1^f = x_1^i = x_1^*$, and either $x_2^i = 0$ and $x_2^f = x_2^*$, or $x_2^i = x_2^*$ and $x_2^f = \varepsilon$ for ε small. These two cases correspond to the addition or the removal of CPA, respectively. In the second case, theoretically, one must set $x^f = (x_1^*, \varepsilon)$ because the dynamics of the system only allow an asymptotic approach to the x_1-axis. Furthermore, we assume the bounds $0 \leq M_1(t) \leq \bar{M}_1$ and $0 \leq M_2(t) \leq \bar{M}_2$, where $\bar{M}_i$ are maximal physical or practical concentration limits (e.g. $\bar{M}_1$ may be limited by the salt or sucrose saturation point and $\bar{M}_2$ may be limited by a maximum practical viscosity), and because of natural equilibration constraints of the system (cf. [7]) we restrict x^i and x^f so that $x_2^y < x_1^y \bar{M}_2$ and $x_{np} > x_1^y \bar{M}_1$ ($y = i$ or f).

We define ϕ_t^λ to be the solution of (3) with control $M = \lambda$ at a time t and the initial condition $\phi_0^\lambda(x) = x$. Also we define the curves $\sigma^j := \{x \in (\mathbb{R}^+)^2 : x \in \phi_t^{M^j}(x^f), t < 0\}$, for

$j = I, II$, and III, the time $\tau > 0$ to be the first time that $\phi_\tau \in \sigma^j$, and the time $t^* > 0$ to be the total time required to reach x^f. In [7] we synthesized optimal controls based on the Pontryagin Maximum Principle (PMP) [30] and proved optimality based on a theorem of Boltayanski [8] but did not provide an explicit example or show how to incorporate constraints.

For the unconstrained case, the optimal CPA addition and removal controls, respectively, are given by

$$M_A(t) = \begin{cases} M^I, & t \leq \tau, \\ M^{II}, & \tau < t < t^*, \end{cases} \quad \text{and} \quad M_R(t) = \begin{cases} M^{III}, & t \leq \tau, \\ M^{II}, & \tau < t < t^*. \end{cases}$$

While these controls are optimal, they come at the cost of possibly excessive volume excursions (see Fig. 2). To remedy this possibility, we will optimize in the presence of constraints, which correspond to lines in the state space

$$\ell_* := \{(x_1, x_2) \in (\mathbb{R}^+)^2 : \gamma x_2 = -x_1 + k_*\} \tag{7}$$

and

$$\ell^* := \{(x_1, x_2) \in (\mathbb{R}^+)^2 : \gamma_2 x_2 = -x_1 + k^*\}. \tag{8}$$

In practice, if $\bar{M}_1$ and $\bar{M}_2$ are large enough, it is enough to only use constraints of the form $k_* \leq x_1 + \gamma_2 x_2$ for both CPA addition and removal protocols. We state this in a lemma which follows directly from the derivation of equations (9) and (13) below.

Lemma 1 *In the CPA addition case, where* $x^i = (x_1(0), 0)$, $x^f = (x_1(0), \eta)$, $\eta > 0$, *and* $\Gamma \cdot x^i < k^*$, *if* $\bar{M}_2 > \frac{(1 - \gamma_2 b)\eta + x_{np}}{(1 - b\gamma_2)x_1^i}$, *then* $\phi_t^{M^I}(x^i) \cap \ell^* = \emptyset$. *In the CPA removal case, where* $x^i = (x_1(0), \eta)$, $x^f = (x_1(0), \varepsilon)$, ε *small, and* $\Gamma \cdot x^i < k^*$, *if* $\bar{M}_1 > \frac{(1 - b\gamma_2)\eta + x_{np}}{k^* - \gamma_2 \eta}$, *then* $\phi_t^{M^{III}}(x^i) \cap \ell^* = \emptyset$.

In both addition and removal cases we will define at most three times $t_1 < t_2$ and τ corresponding to the switching times for control schemes. Note that these are times

in the transformed space; we must use the $s = q(t)$ function in display (2) to determine "real" switching times. There are three possibilities to the dynamics of the optimal control problem: 1) the state constraint is inactive and the bang-bang optimal control outlined above is optimal; 2) the state constraint is active but $\phi_t^\lambda(x^f) \notin \ell_*$ for all $t \leq \tau - t^*$; 3) the state constraint is active and $\phi_t^\lambda(x^f) \in \ell_*$ for some $t \leq \tau - t^*$. These cases are shown in figure (2). Because of the above argument, it follows that in cases (2) and (3) there are times t_1 and t_2 where the unconstrained optimal path intersects the constraint line. The constrained Pontryagin Maximum Principal states that if the optimal control M exists, there is a costate variable p such that for $t \in (t_1, t_2)$, $M \in \mathscr{A}$ maximizes the Hamiltonian $H(x, p, M) := f(x, M) \cdot p + x_1$, and that the constraint remains active. Moreover, we must have the jump condition $\lim_{t \to t_1^+} p(t) = \lim_{t \to t_1^-} p(t)$. Using this fact, we are able to deduce the optimal controls. For $t \notin (t_1, t_2)$ the controls are the same as for the unconstrained system. For $t \in (t_1, t_2)$, we must maximize $H(x, p, M)$ with $\gamma_2 x_2 = -x_1 + k_*$, which is equivalent to maximizing

$$\max_{M_1, M_2} \left\{ -M_1 p_1 (k_* - \gamma_2 x_2) + M_2 (b p_2 - p_1)(k_* - \gamma_2 x_2) \right\}.$$

Derivation of CPA addition optimal controls with an active constraint

In the CPA addition case, from our previous analysis [7] $p_1(t_1) > 0$ and $p_2(t_1) > p_1(t_1)/b$, so $p_1(t_1)$ and $p_2(t_1)$ are both positive. Thus, since $k_* - \gamma_2 x_2 > 0$, we must choose M_1 as small as possible and M_2 as large as possible with the active constraint. Thus, if $\bar{M}_2$ is large in the sense of Lemma 1, we may set $M_1 \equiv 0$. Because of this, we can explicitly solve system (3) with $\Gamma \cdot x = k_*$ for $M_2(t)$. To do so, note $\Gamma \cdot \dot{x} = 0$, which means we have $\dot{x}_1 = -\gamma_2 \dot{x}_2$, or

$$-M_2 x_1 + x_2 + x_{\mathrm{np}} = -\gamma_2 (M_2 b x_1 - b x_2),$$

which we solve for

$$M_2 = \frac{(1 - \gamma_2 b)x_2 + x_{\text{np}}}{(1 - b\gamma_2)x_1}, \tag{9}$$

and substitute this back into the system (3) with $M_1 = 0$ to get

$$\dot{x}_1 = \gamma_2 b x_{\text{np}}/(b\gamma_2 - 1),$$
$$\dot{x}_2 = b x_{\text{np}}/(1 - b\gamma_2). \tag{10}$$

This system has the solution $x = (x_1, x_2)$ given by

$$x_1(t) = \gamma_2(t - t_1)b x_{\text{np}}/(b\gamma_2 - 1) + x_1(t_1)$$

$$x_2(t) = b x_{\text{np}}(t - t_1)/(1 - b\gamma_2) + x_2(t_1).$$

Substituting these solutions into (9) and simplifying, we determine the constrained optimal

CPA addition control

$$M_2^A(t) = \frac{(1 - b\gamma_2)x_2(t_1) + (1 + bt)x_{\text{np}}}{(1 - b2\gamma_2)x_1(t_1) - b\gamma_2 x_{\text{np}}t}. \tag{11}$$

Thus for Case (1) we have one switching time, τ, for Case (2) we have switches $t_1 <$
$t_2 < \tau$, and for Case (3) we have switches $t_1 < t_2$. With these switching times we can define
the optimal controls in each scheme. For all three cases $M_1(t) \equiv 0$, and in Case (1-3), we
have

$$
\begin{array}{ccc}
\text{Case (1)} & \text{Case (2)} & \text{Case (3)}
\end{array}
$$

$$
M_2(t) =
\begin{cases}
\bar{M}_2, & t \le \tau, \\
0 & \tau < t < t^*
\end{cases}
,
\begin{cases}
\bar{M}_2, & t \le t_1, \\
M_2^A(t), & t_1 < t < t_2, \\
\bar{M}_2, & t_2 < t < \tau, \\
0, & \tau < t < t^*
\end{cases}
,
\begin{cases}
\bar{M}_2, & t \le t_1, \\
M_2^A(t), & t_1 < t < t_2, \\
0, & t_2 < t < t^*.
\end{cases}
\tag{12}
$$

Derivation of CPA removal optimal controls with an active constraint

In the CPA removal case, we previously [7] found that at time t_1, the inequalities $p_1(t_1) < 0$ and $p_2(t_1) < p_1(t_1)/b$ hold, and thus we must maximize $M_1(t)$ and minimize $M_2(t)$. Now, if $\bar{M}_1$ is large in the sense of Lemma 1, we may set $M_2 \equiv 0$. Because of this we can explicitly solve system (3) for $M_1(t)$ as above to obtain

$$M_1 = \frac{x_2(1 - \gamma_2 b) + x_{np}}{x_1}, \tag{13}$$

and upon back substitution, we get

$$\dot{x}_1 = bx_2\gamma_2,$$
$$\dot{x}_2 = -bx_2, \tag{14}$$

which has the solution $x = (x_1, x_2)$ where $x_1(t) = -\gamma_2 x_2(t_1)e^{-bt} + x_1(t_1) + \gamma_2 x_2(t_1)$ and $x_2(t) = x_2(t_1)e^{-bt}$. Substituting this solution into (9) and simplifying, we define the constrained optimal CPA removal control

$$m_1^r(t) = \frac{e^{bt}x_{np} + x_2(t_1) - bx_2(t_1)\gamma_2}{-x_2(t_1)\gamma_2 + e^{bt}(x_1(t_1) + x_2(t_1)\gamma_2)}. \tag{15}$$

For Case (1) we have one switching time, τ. For Case (2) we have switches $t_1 < t_2 < \tau$, and for Case (3) we have switches $t_1 < t_2$. With these switching times we can define the optimal controls in each scheme. For all three cases $m_2(t) \equiv 0$, and in Case (1-3), we have

$$
\begin{array}{ccc}
\text{Case (1)} & \text{Case (2)} & \text{Case (3)}
\end{array}
$$

$$M_1(t) = \begin{cases} \bar{M}_1, & t \leq \tau, \\ 0, & t > \tau \end{cases}, \quad \begin{cases} \bar{M}_1, & t \leq t_1, \\ M_1^r(t), & t_1 < t < t_2, \\ \bar{M}_1, & t_2 < t < \tau, \\ 0, & t > \tau \end{cases}, \quad \begin{cases} \bar{M}_1, & t \leq t_1, \\ M_1^r(t), & t_1 < t < t_2, \\ 0, & t > t_2. \end{cases} \tag{16}$$
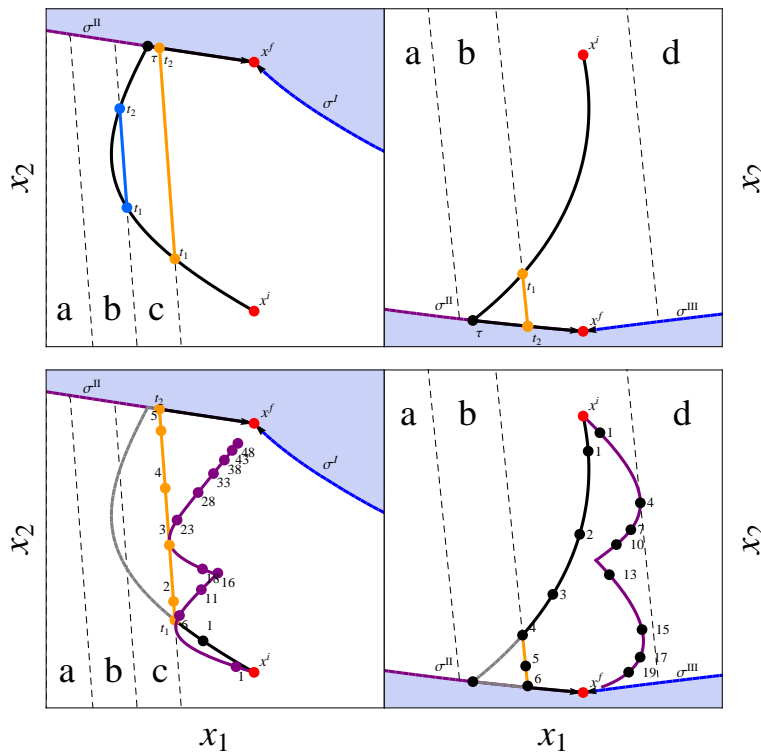
Fig. 2 Plot of system geometry and volume constraints defined by regions *a*, *b*, *c* and *d*. (a) Plot of the optimal CPA addition trajectory in three cases. With constraint level *a* the constraints are inactive, and there is only one switching time τ, and the path is represented by the black line. With constraint level *b*, the unconstrained curve intersects *b* at time t_1 and t_2 and for $t_1 \leq t \leq t_2$ the optimal path is along the constraint boundary, represented by the blue line. With constraint level *c*, the unconstrained curve intersects *c* at time t_1 and t_2, and for $t_1 \leq t \leq t_2$ the optimal path is along the constraint boundary, represented by the orange line. In both latter cases, for $t > t_2$, the optimal trajectory again is the unconstrained curve, represented by the black line. Comparison Plot of optimal (black) and traditional (purple) unconstrained controls; numbers are unitless relative times.

Application of optimal control to human oocyte CPA addition

There are significant advantages to oocyte cryopreservation. It allows women who do not have a reproductive partner to preserve their unfertilized gametes. this becomes especially

relevant to children or women who may undergo potentially sterilizing iatrogenic procedures such as chemotherapy [2]. Nearly 17% of couples experience fertility problems, and the use of cryopreserved embryos significantly reduces the costs associated with treatment [15]. The ethical and legal status of cryopreserved embryos, however, is a significant complication. Successful cryopreservation of oocytes would alleviate these problems and would also provide time for infectious disease screening that is not currently possible.

In the United States, the cost of all *in vitro* fertilization (IVF) and intracytoplasmic sperm injection (ICSI) procedures is nearly $500 million per year, but the indirect costs of the multiple live births associated with multiple embryo transfers is well over $600 million per year [10]. The social and psychological challenges of multiple gestations is also of major concern [3]. one reason multiple embryos are transfered per treatment is that ovarian stimulation and oocyte collection is an invasive and expensive procedure [2]. If oocytes could be sucessfully cryopreserved, multiple oocytes could be harvested and stored until needed. This would facilitate the transfer of single embryos, avoiding the ethical problems of cryopreserving embryos and the patient problems of an invasive and expensive procedure. Transferring single embryos would reduce the overall cost of fertility treatments by half in the united states.

To date, no practical and clinically acceptable cryopreservation protocol exists for human oocytes despite these considerable advantages. Much of the failure is attributed to the sensitivity of the meiotic spindle during CPA addition and removal and while cooling from room temperature to subzero temperatures. Partly to avoid this chilling sensitivity, kuleshova and lopata [22] have argued that vitrification of embryos and oocytes is often favorable to equilibrium (slow) cooling techniques. O'neil et al. [28] have demonstrated that some human oocytes can be successfully vitrified, but the required concentrations of CPA exposes cells to extreme osmotic stresses and potential chemical toxicity due to a lengthy addition and removal procedure. Specifically, to load human oocytes with 6 molar propylene glycol

required for vitrification, 4 steps are needed using a standard protocol taking at least 122 minutes. On the other hand, the osmotic stress can be managed and the effects of chemical toxicity minimized by using the continuous addition protocols developed in this chapter.

Using published parameter values for human oocytes shown in table 3, we compared optimal controls to classic controls for the addition of multimolar (6, 4.16, and 2.46 molar) propylene glycol, with results shown in table 4. Calculations were made with the assumption that the maximal external CPA concentration was 6.5 molar, corresponding to $M_2 = 41$, and a final concentration difference at the highest x_2^f of only 0.5 molar. This value was chosen because at higher concentrations the viscosity of the solution may make the precise control of the extracellular CPA concentration may be impossible. The impact of this concentration constraint can be seen by the relative improvements at each goal concentration level. At the highest goal concentration the improvement ratio values range from 4.7 to 11.1, whereas at the lower concentrations the lowest time improvement is 6.5 and the greatest is 19. Nevertheless, even when $\bar{M}_2 - x_2^f / x_1^f$ is small, the time improvements are at least five-fold.

Sensitivity to parameters

In a biological system with several measured parameters, there will be considerable variation in parameters from one population and even one individual to another. Therefore the implementation of a closed loop optimal control is bound to be subject to errors induced by these variations. We are interested, then, in the effects of these variations on particular endpoints in this protocol, namely, the switching and total times. Additionally, one would expect that there would be cell-to-cell variability in the state constraint as well. This type of problem is easier to "engineer" around: one may simply choose a stricter constraint from the

Table 3 Definition of parameters for oocyte propylene glycol addition

Published and defined parameters[a]	
parameter	value (at 22°c)
L_p [b]	0.53 μm min^{-1} atm^{-1}
P_s	16.68 μm min^{-1}
V^i	2,650,000 μm^3
V_b	503,500 μm^3
V_w^i	2,146,500 μm^3
A	92,539 μm^2
V_*	0.7 $\times v^i$
T	295.15 K

Calculated (unitless) parameters		
Parameter	Equation	Calculated value
b	$P_{s_j}/L_p RTM^{iso}$	4.48
x_1^i	V_w^i/V_w^i	1
x_2^i	$x_1^i c_s^i/M^{iso}$	0
x_1^f	V_w^f/V_w^i	1
x_2^f	$x_1^f c_s^f/M^{iso}$	10.34
k_*	$V_* - V_b/V_w^i$	0.51

[a] All values from [29] unless noted.

[b] Water and solute permeability values published in the literature were determined using a different flux model. to account for this, the conversion was made in a similar manner to that described by [9].

[c] This is about a 44% mass-fraction solution

.

Table 4 Comparison of multimolal CPA addition equilibration times for human oocytes. Several standard protocols with total unitless time t^t, are compared with the optimal constrained protocol. Real times are calculated by multiplying unitless times by $L_p ART M^{iso}/V_w^{iso} = A/V_w^{iso} P_s b_2 = 0.234$. The maximal permeating solute concentration was chosen to be 41, corresponding a 6.5 molar concentration of PG. CPA addition equilibrium steps were determined by calculating the smallest CPA concentration M_2^* such that $x_1 + \gamma_2 x_2 = k_*$, and then following the solution until the switch time equation was satisfied, at which point a new M_2^* was calculated.

x_2^f	switch time equation	t^t	t^t/t^*	actual equilibration time (min)	equilibration steps
36	$x_1(t) = 0.99x_1^i$	522.6	11.12	122.	4
	$x_1(t) = 0.95x_1^i$	281.2	5.98	65.8	4
	$x_1(t) = 0.90x_1^i$	220.2	4.69	51.5	5
20	$x_1(t) = 0.99x_1^i$	374.9	19.4	87.7	4
	$x_1(t) = 0.95x_1^i$	197.3	10.2	46.2	4
	$x_1(t) = 0.90x_1^i$	128.8	6.7	30.1	4
10	$x_1(t) = 0.99x_1^i$	174.9	18.08	40.9	3
	$x_1(t) = 0.95x_1^i$	94.5	9.76	22.1	3
	$x_1(t) = 0.90x_1^i$	62.5	6.45	14.6	3

outset, but we wish to know the effects of moving the state-constraint location on the total transit time.

In the interest of brevity, we will only treat the CPA addition case in which the optimal control follows case (3) of equation (12). Although an analytic expression for the total transit time can be found up to fourth order error terms, this complicated expression involves
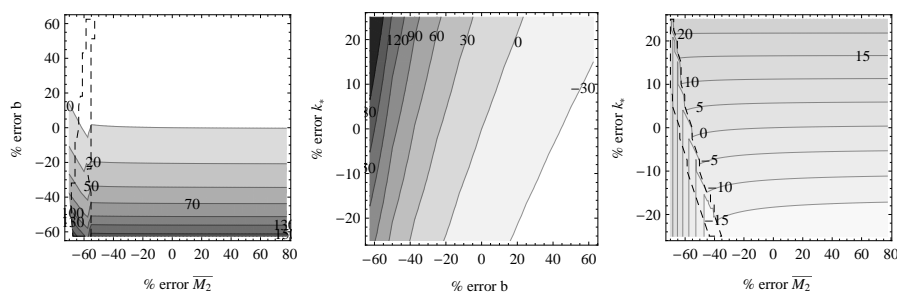
Fig. 3 numerical sensitivity analysis plots. the dashed lines surround the values corresponding to case (2) from display (12). in the case (3) scheme, the error is relatively insensitive to $\bar{m}_2$, but is sensitive to both b and k_*.

multiple special functions, and thus is impractical to use for sensitivity analysis. Therefore we will provide a numerical analysis of the sensitivity to the parameters b, k_*, and $\bar{M}_2$.

The percent error of total time, fixing 1 of the 3 parameters for the respective initial and endpoints $x^i = (1,0)$ and $x^f = (1,1)$ is shown in figure 3. "Correct" parameter values were assumed to be $(b, k_*, \bar{M}_2) = (0.8, 0.8, 5.8)$. The plots are divided into three regions corresponding to the three possible cases, zero, one or two intersections of optimal trajectory with the state constraint. The region contained inside the dashed line corresponds to the case (2) from system (12), the region above and to the right corresponds to case (3) and the region below and to the left corresponds to case (1). For cases (1) and (3) there is a significant effect of maximum concentration, as expected, but for case (2) there is almost no influence of the maximum concentration on the total transit time. This is because the total time to and from the state constraint are small and the total time along the state constratint does not depend explicitly on $\bar{M}_2$.

Discussion and conclusions

Theoretical optimization of cryobiological protocols allows for critical engineering and biological decisions to be made that account for parameter uncertainties in individual cell populations along with imperfect controls. The predictions of this model, with specific, but quite typical parameter values indicate that a significant improvement on the order of 10–20 fold over current techniques is achievable. To put this in perspective, current deglycerolization techniques require 25–30 minutes for the complete process [1]. Using our proposed methods, this protocol should take less than 5 minutes, if optimal controls can be achieved. Unfortunately, accurate estimates of both water and glycerol permeabilities at the wide range of concentrations needed for blood deglycerolization have not been made.

This technique also may be applied to cell types for which standard equilibrium freezing approaches are not sufficient: if extremely high concentrations of CPAs can be equilibrated within the cells, then ultrarapid cooling may "vitrify" both the cells and their surrounding media, achieving a stable amorphous glass. A distinct advantage of this technique is that any x^f may be specified, allowing the control of the amount of dehydration in the final state, yielding even better glass forming tendencies.

In general, even for a large range of temperatures and cell types, $10^{-1} \leq b \leq 10^1$ and $0.5 \leq k_* \leq 0.9$ [5,9]. Because the current "state of the art optimal" CPA addition and removal protocol depends on step-wise (e.g. M_1 and M_2 piecewise constant) protocols, we may compare standard approches to the approach outlined in this manuscript over a very large range of cell types and temperatures. One significant detriment of the traditional approaches is that these produce multiple osmotic events which may have a cumulative damaging effect, but moreover, are difficult to implement as standard laboratory procedures. In Table 5 we show

Table 5 Relative time improvement of the optimized protocols (with total time t^*) over standard protocols (with total time t^t) for a range of unitless parameters and both CPA addition and removal schemes. The number of required equilibrium (standard) steps is also given. In the CPA addition case, $x_2^f = 10$ and in the CPA removal case $x_2^i = 10$. Characteristic maximal concentrations $\bar{M}_1$ and $\bar{M}_2$ were both chosen to be 20. CPA addition equilibrium steps Σ were determined by calculating the smallest CPA concentration M_2^* such that $x_1 + \gamma_2 x_2 = k_*$, and then following the solution until $x_1 = 0.95 x_1^i$, at which point a new M_2^* was calculated. CPA removal equilibrium steps were determined by calculating the largest CPA concentration M_2^* such that $x_1 + \gamma_2 x_2 = k^*$, and then following the solution until $x_1 = 1.03 x_1^i$, at which point a new M_2^* was calculated, except for the last step, when the solution was followed until $x_1 = 1.01 x_1^i$. Note that for CPA removal, the optimal transit time does not depend on k^*.

	Addition of CPA, $x_2^f = 10$					Removal of CPA, $x_2^i = 10$						
b	k_*	t^t	t^*	t^t/t^*	Σ	b	k_*	k^*	t^t	t^*	t^t/t^*	Σ
0.1	0.9	859	79.0	10.9	21	0.1	0.7	1.3	1100	30.0	36.7	17
0.1	0.7	492	59.0	8.33	6	0.1	0.7	1.5	713	30.0	23.7	8
0.1	0.5	399	39.0	10.24	4	0.1	0.7	1.7	569	30.0	18.9	5
1	0.9	84.5	7.86	10.8	14	1	0.7	1.3	107.	3.07	34.9	13
1	0.7	46.5	5.83	7.98	4	1	0.7	1.5	69.9	3.07	22.8	6
1	0.5	40.9	3.80	10.8	3	1	0.7	1.7	55.5	3.07	18.1	4

the relative time improvement of the now protocols over "traditional" protocols, along with the expected step count for the standard approach for each combination of parameters.

This manuscript provides a blueprint for the optimization of cryopreservation protocols, but makes several critical assumptions that must be investigated before implementation in a real-world sense. First, we used an ideal-dilute solution model to facilitate the analytic solution of the optimal control problems. Though mathematically elegant, this assumption may not provide enough accuracy for solutions ranging above 2-3 molal concentrations.

Because of this one may have to choose a suitable non-ideal model for high concentration protocol definition, for example, a simple model that captures much of the non-ideality is one defined by Elliott et al. [12]. Optimal control of systems of this nature is a current area of our research.

Additionally, this protocol depends on the accurate control of the extracellular envirionment immediately adjacent to the cell membrane. In order to implement this control, the extracellular media must be continuously controlled, perhaps by either flowing media over a cell fixed by pipette or membrane [13,27], or by moving the cell through a counter-current, dialysis device [11]. Under both of these conditions, achieving accurate control at the cell membrane boundary involves significant mathematical and engineering effort, with the complications of nonlinear advection and diffusion along with changing viscosities affecting unstirred and boundary layers. These questions were at least partially addressed by Benson [5], with results indicating that at single somatic cell sizes, as long as the membrane surface area remains free, diffusion is sufficient to overcome advective effects, and an ordinary differential equation is most likely sufficient.

References

1. American Association of Blood Banks: Technical manual: 50th anniversary AABB edition 1953-2003. Tech. rep. (2002)

2. American Society for Reproductive Medicine: Patient's fact sheet: Cancer and fertility preservation. Tech. rep. (2003)

3. American Society for Reproductive Medicine: Patient's fact sheet: Challenges of parenting multiples. Tech. rep. (2003)

4. Benson, C.K., Benson, J., Critser, J.: An improved cryopreservation method for a mouse embryonic stem cell line. Cryobiology **56**, 120–130 (2008)

5. Benson, J.D.: Mathematical problems from cryobiology. Ph.D. thesis, University of Missouri (2009)

6. Benson, J.D., Chicone, C.C., Critser, J.K.: Exact solutions of a two parameter flux model and cryobiological applications. Cryobiology **50**(3), 308–316 (2005)

7. Benson, J.D., Chicone, C.C., Critser, J.K.: A general model for the dynamics of cell volume, global stability and optimal control. Journal of Mathematical Biology (In Review)

8. Boltyanskii, V.G.: Sufficient conditions for optimality and the justification of the dynamic programming method. SIAM J. Control **4**, 326–361 (1966)

9. Chuenkhum, S., Cui, Z.: The parameter conversion from the Kedem-Katchalsky model into the two-parameter model. CryoLetters **27**(3), 185–99 (2006)

10. Collins, J., Bustillo, M., Visscher, R., Lawrence, L.: An estimate of the cost of in vitro fertilization services in the United States in 1995. Fertil Steril **64**(3), 538–45 (1995)

11. Ding, W., Yu, J., Woods, E., Heimfeld, S., Gao, D.: Simulation of removing permeable cryoprotective agents from cryopreserved blood with hollow fiber modules. Journal of Membrane Science **288**(1-2), 85–93 (2007)

12. Elliott, J.A.W., Prickett, R., Elmoazzen, H., Porter, K., McGann, L.: A multisolute osmotic virial equation for solutions of interest in biology. Journal of Physical Chemistry B **111**(7), 1775–1785 (2007)

13. Gao, D., Benson, C., Liu, C., McGrath, J., Critser, E., Critser, J.: Development of a novel microperfusion chamber for determination of cell membrane transport properties. Biophys J **71**(1), 443–50 (1996)

14. Gao, D.Y., Liu, J., Liu, C., McGann, L.E., Watson, P.F., Kleinhans, F.W., Mazur, P., Critser, E.S., Critser, J.K.: Prevention of osmotic injury to human spermatozoa during addition and removal of glycerol. Hum Reprod **10**(5), 1109–22 (1995)

15. Garceau, L., Henderson, J., Davis, L., Petrou, S., Henderson, L., McVeigh, E., Barlow, D., Davidson, L.: Economic implications of assisted reproductive techniques: a systematic review. Hum Reprod **17**(12), 3090–109 (2002)

16. Gilmore, J., Liu, J., Gao, D., Critser, J.: Determination of optimal cryoprotectants and procedures for their addition and removal from human spermatozoa. Human Reproduction (1997)

17. Hernández, J.A.: A general model for the dynamics of the cell volume. Bulletin of Mathematical Biology **69**(5), 1631–1648 (2007)

18. Jacobs, M.: The simultaneous measurement of cell permeability to water and to dissolved substances. Journal of Cellular and Comparative Physiology **2**, 427–444 (1932)

19. Karlsson, J.O., Toner, M.: Long-term storage of tissues by cryopreservation: critical issues. Biomaterials **17**(3), 243–56 (1996)

20. Katkov, I.: A two-parameter model of cell membrane permeability for multisolute systems. Cryobiology **40**(1), 64–83 (2000)

21. Kleinhans, F.: Membrane permeability modeling: Kedem-Katchalsky vs a two-parameter formalism. Cryobiology **37**(4), 271–289 (1998)

22. Kuleshova, L., Lopata, A.: Vitrification can be more favorable than slow cooling. Fertil Steril **78**(3), 449–54 (2002)

23. Levin, R., Miller, T.: An optimum method for the introduction or removal of permeable cryoprotectants: isolated cells. Cryobiology **18**(1), 32–48 (1981)

24. Levin, R.L.: A generalized method for the minimization of cellular osmotic stresses and strains during the introduction and removal of permeable cryoprotectants. Journal of Biomechanical Engineering **104**(2), 81–6 (1982)

25. Luyet, B., Gehenio, M.: Life and death at low temperatures. Biodynamica (1940)

26. Mazur, P.: Principles of cryobiology. In: B. Fuller, N. Lane, E. Benson (eds.) Life in the Frozen State, pp. 3–65. CRC Press, Boca Raton, Florida (2004)

27. Mullen, S.F., Li, M., Li, Y., Chen, Z.J., Critser, J.K.: Human oocyte vitrification: the permeability of metaphase II oocytes to water and ethylene glycol and the appliance toward vitrification. Fertility and Sterility **89**(6), 1812–25 (2008)

28. O'Neil, L., Paynter, S., Fuller, B., Shaw, R., DeVries, A.: Vitrification of mature mouse oocytes in a 6 M Me2SO solution supplemented with antifreeze glycoproteins: the effect of temperature. Cryobiology **37**(1), 59–66 (1998)

29. Paynter, S.J., O'Neil, L., Fuller, B.J., Shaw, R.W.: Membrane permeability of human oocytes in the presence of the cryoprotectant propane-1,2-diol. Fertility and Sterility **75**(3), 532–8 (2001)

30. Pontryagin, L.S., Boltyanskii, V.G., Gamkrelidze, R.V., Mishchenko, E.F.: The mathematical theory of optimal processes. Pergamon Press, New York (1962)

31. Woods, E., Benson, J., Agca, Y., Critser, J.: Fundamental cryobiology of reproductive cells and tissues. Cryobiology **48**(2), 146–56 (2004)